calculations, however, occurs in the prediction of the energy levels of the different states. The Serber force calculation gives energy spectra of the 1^-, $T=1$ states in essential agreement with experiment using a strength parameter equal to that for the free nucleon-nucleon interaction. On the other hand for the zero-range force we must use an interaction strength two to three times smaller than the free-particle strength in order to obtain reasonable agreement with the experimental spectrum of oxygen 16. As shown in Ref. 14, this weakening of the interaction is obtained mainly by using the Serber exchange-force mixture, which has no contribution in relative odd angular-momentum states.

ACKNOWLEDGMENTS

I wish to express my gratitude to Dr. John D. Walecka for his patient guidance, enthusiastic encouragement, and critical discussions, which were of invaluable help during the course of this work. I am grateful to Dr. J. Goldemberg for stimulating discussions about this problem, for his help in analyzing the experimental results, and for making available to me experimental data before publication. I am indebted to Dr. L. I. Schiff for his reading and helpful criticizm of the manuscript. Finally I wish to thank Dr. W. Czyz for many interesting discussions.

PHYSICAL REVIEW VOLUME 134, NUMBER 2B 27 APRIL 1964

Studies of Electromagnetic Transitions in N^{14} by Means of the $C^{12}(He^3,p)N^{14}$ Reaction*

E. K. WARBURTON, J. W. OLNESS, D. E. ALBURGER, D. J. BREDIN, AND L. F. CHASE, JR.†
Brookhaven National Laboratory, Upton, New York

(Received 4 December 1963)

The electromagnetic decays of the N^{14} states between 5 and 6.5 MeV were studied using the $C^{12}(He^3,p)N^{14}$ reaction. From investigations of the gamma-ray spectra on and off the 3.0-MeV resonance for production of the N^{14} 6.44-MeV level, this state was found to decay to the ground, 3.95-, and 5.10-MeV levels of N^{14} with branching ratios of $(65\pm3\%)$, $(21\pm2)\%$, $(14\pm3)\%$, respectively. From a study of the internal pairs corresponding to the $6.21\rightarrow2.31$ transition, this transition was shown to be predominantly $M1$ so that the N^{14} 6.21-MeV level has even parity. Similarly, it was confirmed that the N^{14} $6.44\rightarrow0$ transition is predominantly $E2$. The angular distributions of the gamma rays from $C^{12}+He^3$ at $E_{He^3}=2.75$ MeV were measured. It was shown that the mixing parameter x (amplitude ratio of quadrupole to dipole radiation) for the $5.69\rightarrow0$ transition is $x=+0.03\pm0.03$ and for the $5.10\rightarrow0$ transition $x=-0.12\pm0.03$. The branching ratios of the N^{14} 5.10-, 5.69-, and 6.21-MeV levels to the N^{14} ground state and 2.31-MeV first excited state were measured. The results are in satisfactory agreement with previous determinations.

I. INTRODUCTION

ELECTROMAGNETIC transitions in N^{14} have recently been investigated at this laboratory using the $C^{13}(d,n)N^{14}$ reaction.[1,2] It was found that at the deuteron energies used (1.9–3.1 MeV) the N^{14} 6.21-MeV level was excited quite weakly, so that the gamma rays from the decay of this state were not observed. The ground-state transition from the N^{14} 6.44-MeV level was observed, but the state was excited so weakly as to make it difficult to study transitions from this level via the $C^{13}(d,n)N^{14}$ reaction.

Recent work at Rice[3] has shown that the 6.21- and 6.44-MeV levels of N^{14} are produced in the $C^{12}(He^3,p)N^{14}$ reaction, at a bombarding energy of 3 MeV, with cross sections comparable to those of the lower excited states of N^{14}. There is, in fact, a strong resonance with a laboratory width $\Gamma=(125\pm10)$ keV for the production of the 6.44-MeV level (but not the 6.21-MeV level) at $E_{He^3}=2.99$ MeV[3], and the presence of this resonance greatly facilitates a study of the electromagnetic transitions from the 6.44-MeV level. Furthermore, the only gamma rays with energies greater than 2.5 MeV which are expected from $C^{12}+He^3$ at 3-MeV bombarding energy are those from the $C^{12}(He^3,p)N^{14}$ reaction ($Q=4.77$ MeV). This lack of competing reactions is in contrast to a study of N^{14} transitions via $C^{13}+d$ where interfering radiations arise from the $C^{13}(d,p)C^{14}$ reaction.

One purpose of this investigation, then, was to study the electromagnetic transitions from the decay of the N^{14} levels at 6.21 and 6.44 MeV. For the former level the decay modes are known and our aim was to determine the parity of this level which was not definitely established when this work was started.[4] For the

* Work performed under the auspices of the U. S. Atomic Energy Commission.
† Permanent address: Lockheed Missiles and Space Laboratory, Palo Alto, California.
[1] D. E. Alburger and E. K. Warburton, Phys. Rev. **132**, 790 (1963).
[2] E. K. Warburton, D. E. Alburger, A. Gallmann, P. Wagner, and L. F. Chase, Jr., Phys. Rev. **133**, B42 (1964).
[3] H. Kuan, T. A. Belote, J. R. Risser, and T. W. Bonner, Bull. Am. Phys. Soc. **8**, 125 (1963); and H. Kuan (private communication).
[4] F. Ajzenberg-Selove and T. Lauritsen, Nucl. Phys. **11**, 1 (1959).

6.44-MeV level, the work of Kuan *et al.*[3] has led to the assignment $J^\pi = 3^+$ and the purpose of this investigation was to establish a decay scheme for this level—the only established decay mode at present being to the N^{14} ground state.[4]

The N^{14} 5.10-, 5.69-, and 6.21-MeV levels all decay to both the 1^+ N^{14} ground state and to the 0^+ N^{14} first excited state at 2.31 MeV. As will be shown in Sec. IV this means that the mixing parameter x (the amplitude ratio of quadrupole to dipole radiation) in the ground-state transitions can, in principle, be determined from measurements of the angular distributions of both decay modes. The accuracy with which this determination can be made is directly dependent on the degree of alignment of the levels. Previous work[5] on the $C^{12}(He^3,p)N^{14}$ reaction indicates that in this reaction the excited states of N^{14} are quite strongly aligned, i.e., the angular distributions of the gamma rays are strongly anisotropic. Thus, it would seem that the $C^{12}(He^3,p)N^{14}$ reaction is a good one to use to test this method for determining the mixing parameter x.

II. DECAY SCHEME OF THE N^{14} 6.44-MeV LEVEL

A. Three-Crystal Pair Spectra

The N^{14} 6.44-MeV level decays predominantly to the ground state with a suspected branch to the 3.95-MeV level.[6] In order to search for the $6.44 \rightarrow 3.95$ gamma ray of 2.49 MeV and other possible modes of decay, three-crystal pair spectra were recorded for a He^3 beam incident on a C^{12} target which was $\sim$250 keV thick for 3.0-MeV He^3 ions. The spectra were taken for beam energies of 2.75, 2.9, 3.0, 3.1, and 3.5 MeV with the center crystal of the three-crystal pair spectrometer at 35° to the He^3 beam. The center NaI crystal was 1.5 in. in diam and 3 in. long, while the two side crystals were both 3 in. in diam and 3 in. long. The front face of the center crystal was 5.2 in. from the target. A collimator consisting of a 0.65-in. diam hole in a 3.6-in.-thick lead brick was placed 1.5 in. from the center crystal. A Cosmic Radiation Laboratory Model 801 multiple-coincidence unit provided the triple coincidence conditions. The output from the center crystal was displayed with a RIDL 400-channel analyzer. The spectra obtained at beam energies of 2.9 and 3.1 MeV are illustrated in Fig. 1. All the peaks shown except that from the $C^{12}(He^3,\alpha)C^{11}(2.00 \rightarrow 0)$ reaction are assigned to transitions in N^{14}. The peaks are labeled [in Fig. 1(a)] by the energies of the initial and final states of the transitions to which they belong.

The solid curves of Fig. 1 are the results of a least-squares computer fit to the measured spectra. The program was obtained through the courtesy of H. T. Motz of Los Alamos, who has adapted a Gaussian peak

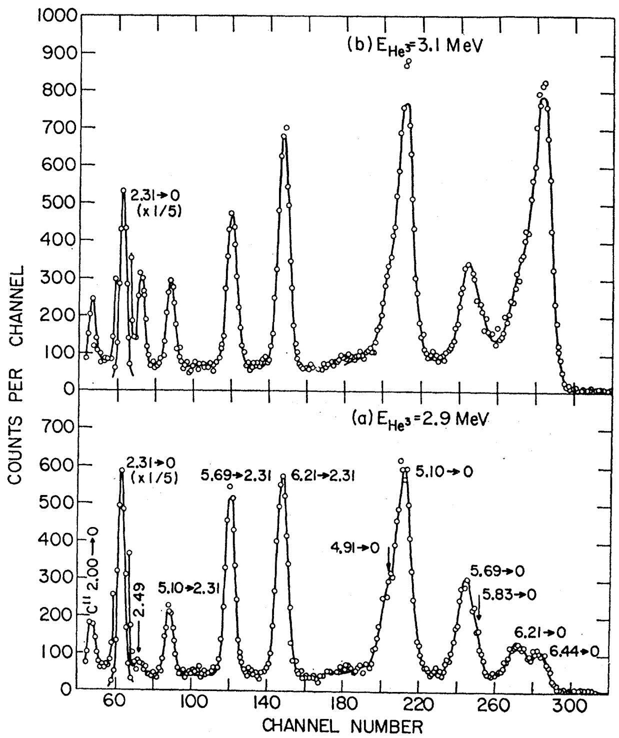

FIG. 1. Three-crystal pair spectra of the gamma rays from a $\sim$250-keV thick C^{12} target bombarded by (a) 2.9-MeV He^3 ions and (b) 3.1-MeV He^3 ions. The center crystal of the spectrometer was placed at 35° to the He^3 beam. The solid curve is a computer fit (see text) to the experimental data (open circles). All the peaks are assigned to transitions in N^{14} except for the one corresponding to the C^{11} $2.00 \rightarrow 0$ transition. The peaks are identified in (a) by the energies in MeV of the N^{14} initial and final states of the transitions to which they are assigned.

fitting program[7] for use in the analysis of three-crystal pair spectra. In the Motz program, the individual gamma-ray lines are represented as being the sum of a Gaussian peak and an exponential tail, the latter arising primarily from bremsstrahlung losses in the center crystal.

As an illustration of the procedure we have shown in Fig. 2, the fit obtained for the 6.13-MeV line from $F^{19}(p,\alpha\gamma)O^{16}$. The experimental data were obtained by recording the gamma-ray spectrum at a resonance where the 6.13-MeV line predominates; additional measurements at two other resonances permitted the straightforward subtraction of contributions from the weaker higher lying lines at 6.9 and 7.1 MeV, yielding the corrected spectrum shown. The computed spectrum is shown by the solid line; its resolution into Gaussian and exponential components is indicated.

The functional form used in the computer fit is given by

$$Y(E)=\frac{A}{(2\pi)^{1/2}\sigma}e^{-\frac{1}{2}(\zeta^2/\sigma^2)}+CAe^{-D\zeta}\{1-e^{-\frac{1}{2}(\zeta G)^2}\},$$

---

[5] D. A. Bromley, E. Almqvist, H. E. Gove, A. E. Litherland, E. B. Paul, and A. J. Ferguson, Phys. Rev. **105**, 957 (1957).

[6] H. J. Rose, Nucl. Phys. **19**, 113 (1960).

[7] P. McWilliams, W. S. Hall, and H. E. Wegner, Rev. Sci. Instr. **33**, 70 (1962).

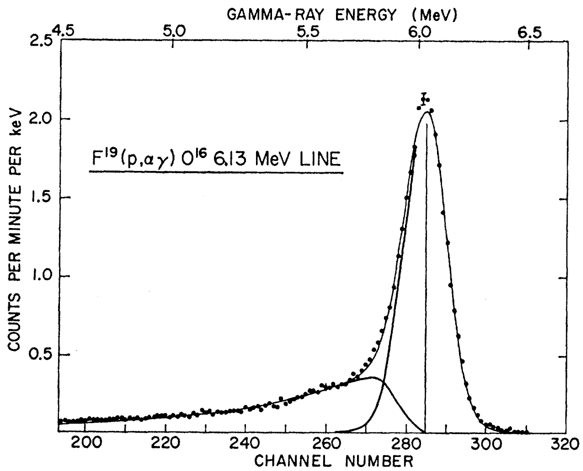

FIG. 2. Three-crystal pair spectra of the O^{16} 6.13 → 0 transition produced by the reaction F^{19} $(p,\alpha\gamma)O^{16}$. The procedure for obtaining the experimental spectrum (solid points) is explained in the text. A least-squares fit of the function $Y(E)$ defined in the text is given by the solid curve; its resolution into Gaussian and exponential components is indicated. Values thus determined for the parameters describing the Gaussian peak are listed: $\sigma=96.3$ keV; $E_{\gamma 0}=6{,}137$ keV; and $A=473$ counts/min. The tail parameters are $C=1.12\times10^{-3}$ and $D=-1.46\times10^{-3}$.

where $\zeta=E-E_{\gamma 0}$. The first term yields the Gaussian peak at $E_{\gamma 0}$, characterized by the width σ and area A. The second term is set to zero for $\zeta>0$, and describes the exponential tail of amplitude CA and slope D. The constant G is chosen to round off the exponential in the peak region, thus avoiding discontinuities in the final line shape. Values of the parameters σ, A, $E_{\gamma 0}$, C, and D for the 6.13-MeV line are given in the caption of Fig. 2.

It is evident from Fig. 2 that the computed curve fails to match the datum points in the region of the peak maximum. An examination of this feature indicates that the mismatch occurs because the experimental peak is not accurately represented by a pure Gaussian. In order to fit the peak at its extremities, the program requires a value for σ somewhat larger than that required for just the central region: The resultant curve is therefore obtained as a compromise between these extreme values.

In terms of area, the extent of the mismatch is about 1.5%. Similar results are obtained for various other lines. In the following, however, we shall be concerned primarily with the *ratios* of peak areas, and hence, the above errors do not significantly affect the results of these calculations.

Similar fits were obtained for a number of single-line spectra in the region $2.5\leq E_{\gamma 0}\leq 7.1$ MeV. In this way the characteristics of the three-crystal pair spectrometer were investigated, and the energy dependences of the shape parameters σ, C, and D were determined. One parameter of interest which was determined from these spectra is the ratio of the number of counts in the Gaussian peak (Σ_G) to the total number of counts in the pair line (Σ_T). This ratio is given as a function of gamma-ray energy in Fig. 3.

For the six higher lying lines of Fig. 1, values for C and D were taken directly from the work described above, and were held fixed throughout the calculation. Values for σ were adjusted slightly to conform to the resolution actually obtained in this particular measurement. Hence the computer was left with the problem of determining simply peak positions and areas. Although the program is, in principle, capable of handling in a given run as many as eight peaks, each with five parameters, the work involved in obtaining a final solution is considerably simplified though the adoption of the above approach. This problem has been discussed further elsewhere.[7]

For the lower lying lines, the bremsstrahlung tails are quite small, and hence were neglected; the data were analyzed by fitting simple Gaussian peaks superimposed on a flat background. In this case the exponential tails of the peaks are absorbed into the background which arises mainly from the tails of the higher energy lines.

The peak areas obtained from the computer fit to the spectra of Fig. 1 were converted to relative gamma-ray intensities, I_γ, using the relationship

$$I_\gamma \propto \frac{\Sigma_G}{(\Sigma_G/\Sigma_T)\sigma_p},$$

where Σ_G is the area in the Gaussian peak for a given pair line and (Σ_G/Σ_T) is the peak-to-total ratio obtained from Fig. 3. σ_p is a factor describing the energy dependence of the pair production cross section, and incorporates corrections for the finite length of the center crystal and for losses due to annihilation in flight. The results are given in Table I. Transition energies are the averages of those obtained from the least-squares fit with the gamma rays at (5.104 ± 0.010) MeV and (2.331 ± 0.001) MeV used for calibration. The energies of these calibration lines are the best values[4] for the

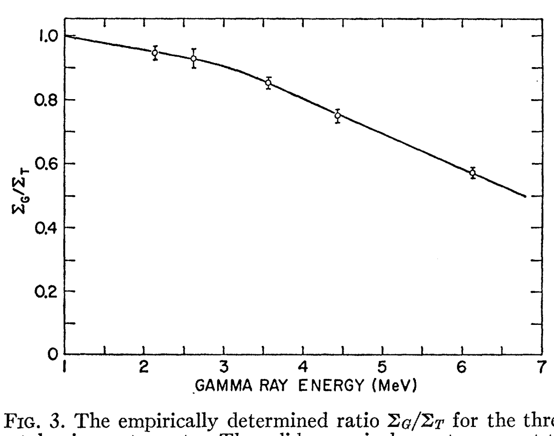

FIG. 3. The empirically determined ratio Σ_G/Σ_T for the three-crystal pair spectrometer. The solid curve is drawn to connect the experimental points. Σ_T is the total area under a given monoenergetic gamma-ray line and Σ_G is the area under the Gaussian peak (see Fig. 2).

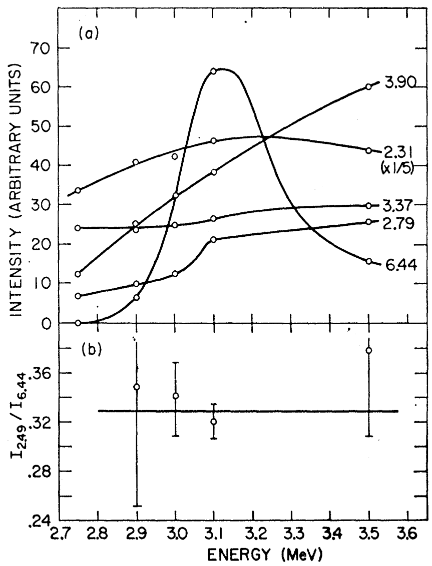

FIG. 4. (a) Yield versus He^3 beam energy for various gamma rays from the $C^{12}(He^3,p)N^{14}$ reaction. The curves are identified by the energies in MeV of the gamma rays to which they correspond. (b) Ratio of the intensities of the 2.49-MeV N^{14} 6.44 → 3.95 transition and the 6.44-MeV N^{14} 6.44 → 0 transition versus He^3 beam energy.

excitation energies of the initial states of these ground-state decays. A 0.8% Doppler shift was added to the energy of the 2.331-MeV peak since this transition has the full Doppler shift expected from the kinematics,[4] while a zero Doppler shift was assumed for the N^{14} 5.10 → 0 transition since the measured Doppler shift of this transition is zero within the errors.[4] The energies listed in Table I are uncorrected for Doppler shifts and thus, depending on the lifetimes of the initial states they should be up to 1% higher than the transition energies calculated from the differences in energies of the initial and final states.

Relative intensities were also obtained for the 6.44-MeV peak and for the gamma rays with energies less

TABLE I. Relative intensities of the N^{14} gamma rays observed with a three-crystal pair spectrometer at 35° to the beam from the bombardment of a C^{12} target, 250 keV thick for 3.0-MeV He^3 ions, by 2.9- and 3.1-MeV He^3 beams.

E_γ(MeV)[a]	Assignment	Relative Intensity (Arbitrary Units) $E_{He^3}=2.9$ MeV	$E_{He^3}=3.1$ MeV
6.444±0.02	6.44 → 0	6.5±0.4	63.7±3
6.231±0.03	6.21 → 0	6.9±0.4	16.3±6
5.865±0.06	5.83 → 0	3.1±0.6	2.7±1.3
5.716±0.02	5.69 → 0	14.6±0.8	17.8±1.6
(5.104±0.01)	5.10 → 0	28.8±1.5	49.0±3
4.954±0.02	4.91 → 0	9.0±2	13.2±5
3.907±0.01	6.21 → 2.31	25.2±1.4	38.2±2
3.400±0.006	5.69 → 2.31	23.8±1.4	27.6±2
2.805±0.005	5.10 → 2.31	9.8±1	17.3±1
2.509±0.003	6.44 → 3.95	2.4±0.8	21.0±1
(2.331±0.001)	2.31 → 0	204 ±9	232 ±10

[a] Average of the values obtained at 2.9 and 3.1 MeV uncorrected for Doppler shifts. The energies in parenthesis were used for calibration.

than 4 MeV from the pair spectra taken at five bombarding energies ranging from 2.75 and 3.5 MeV. The excitation curves obtained from these results are shown in Fig. 4(a). The effect of the strong resonance in the $C^{12}(He^3,p)N^{14}$ reaction for formation of the 6.44-MeV level at $E_{He^3}=2.990\pm0.010$ MeV[3], is apparent in Fig. 4(a). The line drawn through the points for the 6.44-MeV data is a rough sketch of the excitation curve expected for a resonance at $E_{He^3}=2.99$ MeV with a width in the laboratory system of 125 keV.[3] The excitation curve for the 2.79-MeV gamma ray from the N^{14} 5.10 → 2.31 transition also may be influenced by this resonance. None of the other excitation curves gives an indication of the resonance within the uncertainties of the measurements. The gamma ray with a measured energy of (2.509±0.003) MeV (2.49 MeV after correction of 20 keV assuming the full Doppler shift) observed in the $E_{He^3}=3.1$-MeV pair spectrum [Fig. 1(b)] has the right energy to be associated with the N^{14} 6.44 → 3.95 transition. In fact, a gamma ray of this energy cannot be assigned to a transition between any of the known states in N^{14}, O^{14}, or C^{11} which can be excited by a 3.1-MeV He^3 beam. Furthermore, the 2.49-MeV gamma ray exhibits the same resonance behavior as the 6.44-MeV gamma ray. This is illustrated in Fig. 4(b) where the ratio of the 2.49- and 6.44-MeV gamma rays are plotted against beam energy. We conclude that the 2.49-MeV gamma ray is due to the N^{14} 6.44 → 3.95 cascade, confirming the earlier tentative identification of this cascade.[6]

The N^{14} 6.44-MeV level has been assigned $J^\pi=3^+$ from an investigation of the 2.99-MeV resonance in $C^{12}+He^3$. Thus, we expect that the transitions to the N^{14} ground state and 3.95-MeV level (both of which have $J^\pi=1^+$) are both $E2$. Significant admixtures of $M3$ radiation in either transition are considered unlikely, especially because of the inhibition of $\Delta T=0$ Ml transitions in self-conjugate nuclei.[8] The angular distribution of the 6.44 → 0 transition at the 2.99-MeV resonance in the $C^{12}(He^3,p)N^{14}$ reaction was measured by Kuan *et al.*[3] and was found to be in good agreement with the distribution $W(\theta)=1+0.49P_2(\cos\theta)-0.30P_4(\cos\theta)$, which is expected for the resonance parameters, $l_{He^3}=2$, $l_p=0$, $J_{res}{}^\pi=\frac{5}{2}^+$ with $J^\pi=3^+$ for the N^{14} 6.44-MeV level, and assuming that the 6.44 → 0 transition is pure $E2$. These resonance parameters are in agreement with other aspects of the investigation of the resonance made by Kuan *et al.* Thus, we expect the same distribution for the 2.49-MeV 6.44 → 3.95 transition at resonance, and a measurement of this distribution would be a check on the assignment of the 2.49-MeV gamma ray to the N^{14} 6.44 → 3.95 transition. For this reason, angular distributions of the gamma rays from $C^{12}+He^3$ were measured at $E_{He^3}=3.1$ MeV by recording three-crystal pair spectra at angles to the beam of 0°, 28°, 42°, 55°, and 90°. Gamma-ray intensi-

[8] E. K. Warburton, Phys. Rev. Letters 1, 68 (1958).

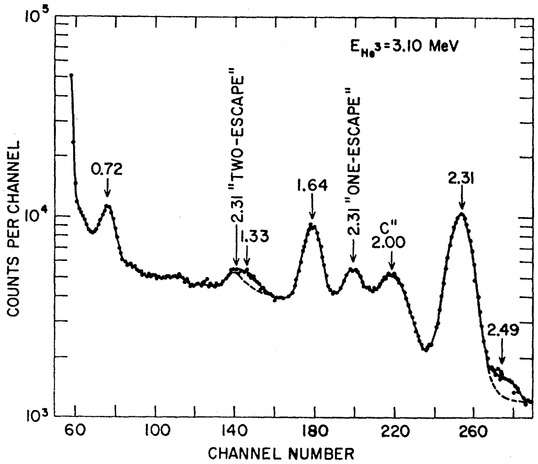

FIG. 5. The points and solid curve show the singles spectrum of gamma rays from $C^{12}+He^3$ at $E_{He^3}=3.10$ MeV obtained with a 3×3-in. NaI(Tl) crystal. The N^{14} peaks are identified by their energies in MeV. One C^{11} transition is also shown. The shape of the singles spectrum near 1.32 and 2.49 MeV obtained at $E_{He^3}=2.9$ MeV is indicated by the dashed curves which are normalized to the solid curve in the energy regions just above and just below the indicated dashed curves.

ties at each angle were obtained from the areas in the Gaussian peak by using the same computer fitting procedure as for the spectra of Fig. 1. The efficiency of the three-crystal spectrometer had been found to vary somewhat with the angle at which it was placed, to the extent of about 5%; therefore, the angular distributions were obtained by normalizing the peak areas to that of the N^{14} 2.31 → 0 transition, which is isotropic by virtue of the zero spin of the N^{14} 2.31-MeV level.[4] The angular distributions of the various gamma rays were fitted by the least-squares method to the expression $W(\theta)=1+A_2P_2(\cos\theta)+A_4P_4(\cos\theta)$. For the 6.44- and 2.49-MeV gamma rays, the results are $A_2=+(0.54\pm0.1)$, $A_4=-(0.2\pm0.1)$, and $A_2=+(0.45\pm0.07)$, $A_4=-(0.25\pm0.07)$, respectively. These two distributions are in good agreement with each other and with the expected distribution which has, allowing for effects of the finite detector size, $A_2=+0.49$ and $A_4=-0.29$. Thus, the angular distribution measurement confirms the assignment of the 2.49-MeV gamma ray to the N^{14} 6.44 → 3.95 transition.

The ratio of the yields of the 2.49- and 6.44-MeV gamma rays was obtained from the data shown in Fig. 4(b), and from the relative intensities extracted from the three-crystal pair spectra used to obtain the angular distributions. An intensity ratio $I_{2.49}/I_{6.44}=(0.32\pm0.02)$ was obtained from the average of the various measurements.

B. Coincidence Spectra

The excitation curve given in Fig. 4(a) for the 2.79-MeV gamma ray shows a possible influence of the 2.99-MeV resonance. If so, this could very well be due to the N^{14} 6.44 → 5.10 → 2.31 cascade in which case a 1.33-MeV gamma ray would be involved. Some evidence for such a gamma ray was seen in singles spectra taken with a 3×3-in. NaI crystal 2 in. from the target and at 90° to the beam. A singles spectrum taken at $E_{He^3}=3.1$ MeV is shown by the points and solid curve in Fig. 5. In the region of 1.33 and 2.49 MeV, the dashed curves indicate the normalized spectrum taken at 2.9 MeV. The presence of the resonant 2.49-MeV gamma ray is apparent in Fig. 5, and there is also evidence for a gamma ray with an energy of about 1.33 MeV. All of the other gamma rays identified in Fig. 5 arise from well-known transitions.[4]

The suspected 1.33-MeV gamma ray was looked for by observing the spectra in coincidence with the 5.10-MeV gamma ray corresponding to the ground-state decay (67%) of the N^{14} 5.10-MeV level. Two 3×3-in. NaI crystals were placed on opposite sides of the target with their front faces two in. from it. One of these was used to gate the 400-channel analyzer which displayed the spectrum from the second. Coincidence spectra recorded at $E_{He^3}=2.9$ and 3.1 MeV are shown in Fig. 6. These spectra were taken with the gate set between 4.4 and 5.3 MeV. A gamma ray with an energy of 1.33 MeV is apparent in the 3.1-MeV spectrum but not the 2.9-MeV spectrum. Annihilation radiation arising mainly from the pair production process is responsible for the 0.51-MeV peak. The 0.72-MeV gamma ray is due to the N^{14} 5.83 → 5.10 cascade (85%) while the small 2.31-MeV peak arises from accidental coincidences.

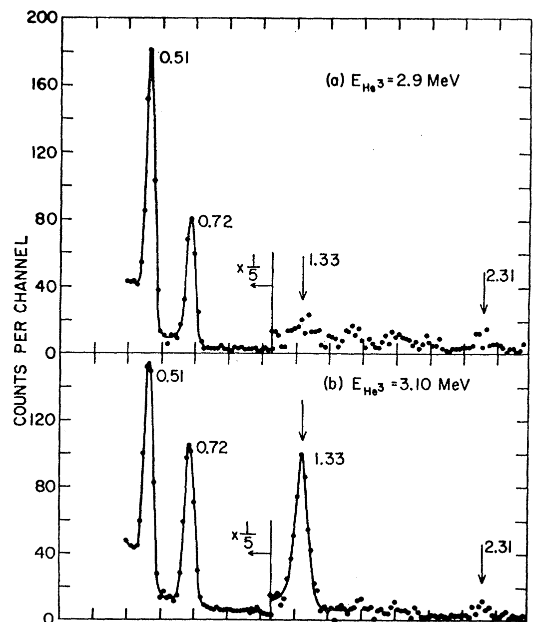

FIG. 6. Coincidence spectra obtained for the gamma rays from $C^{12}+He^3$ at (a) $E_{He^3}=2.9$ MeV and (b) $E_{He^3}=3.1$ MeV. Two 3×3-in. crystals at 90° to the He^3 beam and 2-in. from the C^{12} target were used. The spectra shown are in coincidence with a gate set between 4.4 and 5.3 MeV. The presence of the 2.31-MeV peak is due to random coincidences.

Within the uncertainty with which its energy was measured (±20 keV) the 1.33-MeV gamma ray could belong to a N^{14} 7.03 → 5.69 transition, a N^{14} 6.21 → 4.91 transition, or the N^{14} 6.44 → 5.10 transition. However, the N^{14} 7.03-MeV gamma ray is known to decay predominantly to the N^{14} ground state and so the nonappearance of a 7.03-MeV gamma ray in the three-crystal pair spectra rules out the possibility 7.03 → 5.69. In addition, a coincidence spectrum taken at $E_{He^3}=3.1$ MeV with the gate set from 5.4 to 5.8 MeV showed no sign of the 1.33-MeV gamma ray. The possibility 6.21 → 4.91 is ruled out by the disagreement between the relative yield of the 3.90-MeV gamma ray (6.21 → 2.31 transition) at $E_{He^3}=2.9$ and 3.1 MeV (Fig. 4), and the relative yield of the 1.33-MeV gamma ray at these two energies (Fig. 6). Thus, we assign the 1.33-MeV gamma ray to the N^{14} 6.44 → 5.10 transition.

The intensity of the 1.33-MeV gamma ray relative to that of the 6.44-MeV gamma ray was obtained as follows: The 0.72-MeV gamma ray is also in coincidence with the 5.10-MeV gamma ray, and hence the intensity of the 1.33-MeV gamma ray relative to that of the 2.31-MeV gamma ray could be calculated from the relative intensities of the 0.72- and 1.33-MeV gamma rays in the coincidence spectrum (Fig. 6) and the relative intensities of the 0.72- and 2.31-MeV gamma rays in the singles spectrum (Fig. 5). Then the relative intensities of the 1.33- and 6.44-MeV gamma rays were obtained from the relative intensities of the 2.31- and 6.44-MeV gamma rays (Table I). The result is $I_{1.33}/I_{6.44} = (0.21\pm0.04)$ where the uncertainty includes an estimate of the possible effects of the angular distributions and correlations of the various gamma rays involved.

The $J^\pi=3^-$ 5.83-MeV level is the only remaining known N^{14} level to which the 6.44-MeV level can decay by dipole or $E2$ radiation. Since the 5.83-MeV level decays 85% of the time by cascade to the 5.10-MeV level, a limit can be placed on the intensity of the 0.61-MeV gamma ray associated with the 6.44 → 5.83 transition from the coincidence spectra of Fig. 6(b) and from similar coincidences taken with greater dispersion and statistics.[9] The result can be expressed in the form $I_{0.61}/I_{6.44}<0.04$.

Combining the results given in this section, we have found that the N^{14} 6.44-MeV level decays to the N^{14} ground state, 3.95-MeV level, and 5.10-MeV level with branching ratios of (65±3)%, (21±2)%, and (14±3)% respectively, and that the branch to the N^{14} 5.83-MeV level is <3%.

III. SPIN PARITY OF THE N^{14} 6.21-MeV LEVELS

A. Experimental Procedure

The spin-parity of the N^{14} 6.21-MeV level was determined from a magnetic spectrometer investigation of the multipolarity of the N^{14} 6.21 → 2.31 transition. The theory, design, and test of a spiral baffle system for determining the multipolarities of electromagnetic transitions by measurements in the intermediate-image pair spectrometer has been described previously.[2] An inconvenient mechanical feature of the earlier system was the necessity for breaking the vacuum of the spectrometer in order to install or remove the baffle. In the new arrangement used in the present work a very similar set of baffle blades is attached to a cylindrical mount which can be moved axially inside the spectrometer over a distance of 17 in. At one extreme position, the baffle blades are in the same plane as in the old system, and at the other extreme position, the baffle is completely clear of the trajectories of focused electrons. Another feature of the new system is that the baffle blades are attached to a separate ring that can be rotated with respect to the mount by means of a rack and pinion gear over a total angle of about 120°. Three brass rods of $\frac{3}{8}$ in. diam for moving the baffle axially and a fourth rod for adjusting the baffle azimuthal angle are brought out through "O"-ring seals in the spectrometer end plate. These rods are attached to an external ring having handles for convenience in sliding the baffle axially. The control rod for varying the azimuthal angle of the baffle has a turning handle and an indicating counter which allows the angle to be set with an accuracy of about 2°.

After installing the new system, the position of the detector was adjusted so that the counting rates in the two crystals with the baffle in the "out" position were the same when focusing the K-1.06-MeV conversion electrons from a source of Bi^{207}. In order to establish the proper angle of the baffle with respect to the detecting crystals the upper half of the baffle was temporarily blocked off. Depending on the direction of the magnetic field, the Bi^{207} conversion electrons were then detected (for the baffle "in" position) in only one of the crystals. However, when the baffle was rotated, which had the effect of rotating the image, counts in the opposite crystal were observed starting at a certain "onset angle." This procedure was followed for both directions of the magnetic field and it was found that the "onset" angular positions of the baffle for the two tests differed by 11–12°. The midpoint between these two angles was chosen as the proper and accurate orientation for ratio measurements on pair lines. These tests further confirmed the previous measurement[2] of 225° for the spectrometer rotation angle β, and also showed that one edge of each image coincides quite closely with the junction of the corresponding crystal and the tungsten absorber between the crystals.

Tests of the new baffle system were then made by baffle-in, baffle-out measurements on 7 of the 14 calibration pair lines which had been studied with the old baffle system. The conditions used for producing the calibration lines were the same as in the previous work.[2] The N^{14} 6.44 → 0 transition produced at the 2.99-MeV

[9] J. A. Becker and E. K. Warburton, Phys. Rev. 134, B349 (1964).

TABLE II. Summary of the experimental ratios R_ω' and the corrected ratios R_ω obtained in the present work and the R_ω obtained with the previous baffle system (Ref. 2).

Transition	Multi-polarity	R_ω' (present work)	R_ω (present work)	R_ω (Ref. 2)
C^{13} $3.09\rightarrow 0$	$E1$	0.178 ± 0.006	0.178 ± 0.006	0.185 ± 0.008
Be^{10} $3.37\rightarrow 0$	$E2$	0.133 ± 0.003	0.130 ± 0.004	0.130 ± 0.004
Li^{6} $3.56\rightarrow 0$	$M1$	0.104 ± 0.003	0.104 ± 0.003	0.092 ± 0.002
C^{13} $3.85\rightarrow 0$	$M2$	0.064 ± 0.002	0.063 ± 0.003	0.056 ± 0.005
C^{12} $4.43\rightarrow 0$	$E2$	0.100 ± 0.003	0.097 ± 0.003	0.097 ± 0.005
Be^{10} $5.96\rightarrow 0$	$E1$	0.112 ± 0.002	0.112 ± 0.002	0.102 ± 0.003
O^{16} $6.06\rightarrow 0$	$E0$	0.264 ± 0.003	0.264 ± 0.003	0.265 ± 0.005
N^{14} $6.44\rightarrow 0$	$E2$	0.097 ± 0.005	0.082 ± 0.006	$\cdots$

resonance in $C^{12}+He^3$ was also used for a calibration line. For this work the C^{12} target was identical to that used for the gamma-ray work described in the previous section. During these tests the very considerable advantages of the new system became apparent. The baffle position can be changed in a very short time, usually without removing the beam from the target and with the spectrometer coil current left at a fixed value. Greater accuracy in the measurements is possible since the baffle position can be altered as frequently as desired.

The results of the calibration measurements are summarized in Table II, where the first two columns list the transitions studied and their multipolarities, in the third column are the measured ratios R_ω' of yields ($Y_{\text{with baffle}}/Y_{\text{without baffle}}$) and in the fourth column are the ratios R_ω obtained by applying the correction[2] for alignment of the initial state of the transition. Corrections for alignment for the first 7 transitions of Table II were the same as in the previous work[2] since the conditions used to form the state are identical. In the case of the N^{14} 6.44-MeV transition an alignment correction of 0.85 was calculated from the theoretically predicted coefficients, $A_2=+0.49$, $A_4=-0.30$ appropriate to the 2.99-MeV resonance in $C^{12}+He^3$. The last column of Table II lists the corrected ratios R_ω obtained with the old baffle system.[2]

A comparison of the last two columns of Table II shows that for most of the calibration lines, the two baffle systems give ratios R_ω, which are in agreement. However, for the Li^6 $3.56\rightarrow 0$ and Be^{10} $5.96\rightarrow 0$ transitions the new values of R_ω are about 10% higher than previously measured. The reason for these differences has not yet been established although several explanations are possible. It could be the result of the more precise procedure for aligning the detector and baffle system, or it may be caused by better machining accuracy and other slight differences in the sector angles of the new baffle, which was constructed with greater care than the old baffle. It may also be that other systematic errors inherent in the use of the old baffle system were underestimated. At the present time, the theoretical ratios $R_\omega(l)$ are being renormalized to fit these new measurements. Until that is done, it suffices to adopt empirical correction factors to the previous calibration curves (see Fig. 14 of Ref. 2).

B. Measurement of R_ω for the N^{14} $6.21\rightarrow 2.31$ Transition

The yield of the 3.90-MeV pair line corresponding to the N^{14} $6.21\rightarrow 2.31$ transition (see Fig. 1) was measured with the intermediate-image spectrometer, alternately with and without the baffle in place. The full annulus opening (17 mm) of the spectrometer was used in this measurement. At this annulus opening, the resolution (full width at half-maximum of the pair line) was 3%. The average of four determinations of the ratio R_ω' was 0.100 ± 0.010.

The N^{14} 2.31-MeV level has $J^\pi=0^+$, while the N^{14} 6.21-MeV level has $J=1$.[4] Thus, the $6.21\rightarrow 2.31$ transition is pure $E1$ or $M1$. From the three-crystal pair spectrometer measurements described in the last section, the angular distribution for this transition was obtained and the result for the A_2 coefficient in the expression $w(\theta)=1+A_2P_2(\cos\theta)$ is $A_2=+(0.30\pm0.05)$. For this anisotropy (see Fig. 9 of Ref. 2) the alignment corrections are (1.025 ± 0.005) and (0.88 ± 0.02) for $E1$ and $M1$ assignments, respectively. Thus, the corrected ratios R_ω are 0.103 ± 0.010 and 0.088 ± 0.009 for $E1$ and $M1$ assignments, respectively. The 3.90-MeV pair line also has a contribution from the N^{14} $3.95\rightarrow 0$ transition, but it is known that the 3.95-MeV level decays predominantly to the N^{14} 2.31-MeV level by a 1.64-MeV gamma ray, and has a (3.7 ± 0.6)% branch to the N^{14} ground state.[5] From the relative intensities of the 2.31- and 1.64-MeV gamma rays observed in the singles spectrum (Fig. 5) and from the relative intensities of the 2.31- and 3.90-MeV gamma rays observed in the three-crystal pair spectra (Table I), we estimate that the contribution of the N^{14} $3.95\rightarrow 0$ transition to the 3.90-MeV pair line is 6%. Since the N^{14} $3.95\rightarrow 0$ transition is $M1$, $E2$ or a mixture of both it can be shown that the presence of the N^{14} $3.95\rightarrow 0$ transition has a negligible effect on the experimental ratio R_ω for either an $E1$ or an $M1$ assignment to the N^{14} $6.21\rightarrow 2.31$ transition.

We obtain the theoretically expected ratios $R_\omega(l)$ for a 3.90-MeV transition by normalizing the previously determined $R_\omega(l)$ (which corresponds to a sector angle $\omega=120°$ and a polar angle $\alpha=45.7°$)[2] to the R_ω given in Table II for the present baffle system. At 3.9 MeV the $E1$ curve is unchanged but the $M1$ curve is 10% higher. The predicted ratios $R_\omega(l)$ are $R_\omega(E1)=0.153$, and $R_\omega(M1)=0.090$. It is clear from a comparison between these theoretical values of R_ω and the experimental ratio 0.100 ± 0.010, that the $6.21\rightarrow 2.31$ transition is $M1$ and not $E1$, so that the N^{14} 6.21-MeV level has $J^\pi=1^+$.

We note that the measurement of R_ω for the N^{14}

$6.44 \rightarrow 0$ transition (see Table II) confirms the recent[3] even parity assignment to the $J=3^+$ 6.44-MeV level. Following the procedure described above, the predicted values of $R_\omega(l)$ for a 6.44-MeV transition are 0.035, 0.046, and 0.070 for $M2$, $E3$, and $E2$ assignments, respectively. Although the alignment correction for an $M2$, $E3$ mixture cannot be obtained accurately without knowing the degree of mixing, it can be shown[2] that the correction could not bring agreement between the measured value, $R_\omega'=0.097\pm0.005$, and the theoretical range of values $R_\omega \simeq 0.035-0.046$ for an $M2$, $E3$ mixture. Thus, the transition must be predominantly $E2$. The disagreement between the corrected measured ratio, $R_\omega=0.082\pm0.005$, and the predicted value, $R_\omega(E2)=0.070$, will hopefully be decreased by the renormalization now in progress.

IV. DETERMINATION OF MIXING PARAMETERS FROM ANGULAR DISTRIBUTIONS

A. Theory

In the method introduced by Warburton and Rose[10] and developed further by Litherland and Ferguson[11] the angular distributions and correlations of the gamma rays from an initial state J_i are described in terms of the populations of the m_i substates of that level. In this formalism it is apparent that the mixing parameter x in one transition, $J_i \rightarrow J_f$, can often be determined, given the spins J_i and J_f and the angular distribution of this transition, and of another transition from J_i, for which the spin of the final state and the mixing parameter are known. There are three levels in N^{14} which are formed quite strongly in the $C^{12}(He^3,p)N^{14}$ reaction and which decay to both the N^{14} ground state ($J^\pi=1^+$) and the N^{14} 2.31-MeV level ($J^\pi=0^+$). These levels are those at 5.10-MeV ($J^\pi=2^-$), 5.69-MeV ($J^\pi=1^-$), and 6.23-MeV ($J^\pi=1^+$). All three can decay to the N^{14} ground state by a mixture of dipole and quadrupole radiation and, in principle, the mixing parameters for each of these transitions can be determined from measurements of the angular distributions of the ground-state transition and the transition to the 2.31-MeV level.

Using the method of calculating angular distributions described by Litherland and Ferguson[11] we find the following angular distributions:

For $J_i=1$:[12]

$$W(\theta)=1+F_2(1)P_2(\cos\theta)\,, \tag{1}$$

for $J_f=0$, and

$$W(\theta)=1-\tfrac{1}{2}F_2(1)\frac{1-6x+x^2}{1+x^2}P_2(\cos\theta)\,, \tag{2}$$

for $J_f=1$.

For $J_i=2$:

$$W(\theta)=1-(5/7)F_2(2)P_2(\cos\theta)-(2/7)F_4(2)P_4(\cos\theta)\,, \tag{3}$$

for $J_f=0$, and

$$W(\theta)=1+F_2(2)\frac{0.5+2.236x-0.357x^2}{1+x^2}\times P_2(\cos\theta)+F_4(2)\frac{0.1904x^2}{1+x^2}P_4(\cos\theta) \tag{4}$$

for $J_f=1$.

In these expressions the quantity $F_\nu(J_i)$ is a function of the population coefficients $P(m_i)$ of the initial state, i.e., $F_2(1)=\frac{1}{2}[1-3P(0)]$, $F_2(2)=[1-2P(0)-3P(1)]$, and $F_4(2)=[1+5P(0)-10P(1)]$ with $\Sigma_{mi}P(m_i)=1$. Thus, if we characterize the angular distribution of the transition between the states J_i, J_f by $W(\theta) =\Sigma_\nu A_\nu(J_i,J_f)P_\nu(\cos\theta)$, we can write an equation for the mixing parameter x. For instance, for the case $J_i=J_f=1$

$$(1-6x+x^2)/(1+x^2)=-2A_2(1,1)/A_2(1,0) \tag{5}$$

so that measurements of $A_2(1,1)$ and $A_2(1,0)$ can be used to determine the mixing parameter x if these coefficients are nonzero. Similarly, we have for $J_i=2$, $J_f=1$

$$\frac{1+4.472x-0.714x^2}{1+x^2}=-\frac{10}{7}\frac{A_2(2,1)}{A_2(2,0)}\,,$$

and

$$\frac{x^2}{1+x^2}=-1.5\frac{A_4(2,1)}{A_4(2,0)}\,. \tag{6}$$

We note that the above results are still valid for the case in which either outgoing particle from the reaction used to populate the state J_i is detected in an axially symmetric counter; i.e., symmetric with respect to the incident beam direction. For the special case in which the detector is confined to view a small angular region at 0° or 180° the situation is identical to that designated as method II by Litherland and Ferguson.[11]

B. Angular Distribution Measurements

Three-crystal pair spectra were recorded at a He^3 bombarding energy of 2.75 MeV for angles of observation 0, 30, 45, 60, and 90 deg with respect to the incident beam direction. At the bombarding energy selected, the 6.44-MeV level is not populated to a significant extent. and hence the analysis of the pair spectra becomes somewhat simpler. The target was a thin (~250 keV) carbon foil mounted on a 0.003-in. tantalum backing and placed at 45 deg with respect to the incident He^3 beam, such that gamma rays in the region of observation ($\theta\leq 90°$) passed through the tantalum backing. The beam size was defined by a $\frac{1}{8}$-in. collimator located about 8 in. before the target. While the thickness of the tantalum backing was adequate to completely stop the

[10] E. K. Warburton and H. J. Rose, Phys. Rev. **109**, 1199 (1958).
[11] A. E. Litherland and A. J. Ferguson, Can. J. Phys. **39**, 788 (1961).
[12] The phase for the interference term is that used in Ref. 11 for Ml, $El+1$ mixtures.

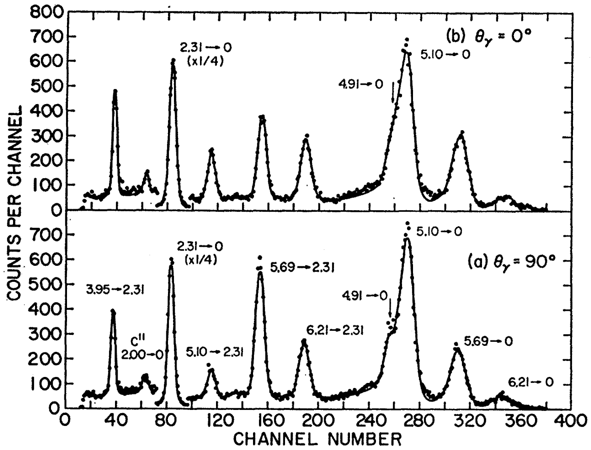

FIG. 7. Three-crystal pair spectra of the gamma rays from a ~250 keV thick C^{12} target bombarded by 2.75-MeV He^3 ions. The center crystal of the spectrometer was placed at (a) 90° to the He^3 beam and (b) 0° to the He^3 beam. The solid curves are computer fits (see text) to the experimental data (solid points). All the peaks are assigned to transitions in N^{14} except for the one corresponding to the O^{11} 2.00 → 0 transition. The peaks are identified in (a) by the energies in MeV of the N^{14} initial and final states of the transitions to which they are assigned.

He^3 beam, it was sufficiently thin as to introduce only negligible absorption corrections into the angular distribution measurements.

A current integrator was used to determine the charge deposited by the beam. In addition, a 3×3-in. NaI detector was used to monitor the reaction gamma rays. The ratio of monitor counts to integrated current remained constant throughout the series of measurements, indicating in particular that there was no measurable deterioration of the carbon target. In order to reduce errors arising from possible angular variations in detection efficiency and geometry, several modifications to the spectrometer apparatus were employed. The three crystals of the spectrometer were fixed in a cylindrical lead casting (7 in. diam×14 in. long) so arranged that the 1.5×3-in. center crystal viewed the target through a horizontal bore along a central diameter of the cylinder. A 2.5-in. lead collimator with a 1-in. aperture was used to define the solid angle of this central detector. The two 3×3-in. side detectors were inserted through 4-in. diam bores along the axis of the cylindrical casting. The entire assembly was cradled on a rotating table which provided for automatic alignment of the central crystal viewing axis on the axis of rotation. For the measurements described here the spectrometer was placed with the face of the central crystal at a distance of 4 in. from the target. Final alignment of the spectrometer with respect to the target was accomplished by placing a point source of Mn^{54} at the target center and then recording the intensity of the 835-keV line as a function of viewing angle. The pivot point of the rotating table was subsequently adjusted (in the horizontal plane) to yield isotropy to within 1%.

The over-all gains of the two side detectors were each stabilized by spectrostats[13] to about 1 part in 500. Weak (~4 μ Ci)Mn^{54} sources were placed near each crystal to provide a constant reference line for this purpose. The windows of the single-channel analyzers of the slow coincidence circuit were then set to encompass ~75% of the counts falling within the photopeak of the 511-keV annihilation line. Through the above procedure, possible variations in the efficiency with which the annihilation quanta of a pair event were detected were reduced to a negligible amount.

In other respects the measurement proceeded in a manner similar to that described previously. Triple coincidences from the fast-slow coincidence circuit were used to gate a 400-channel pulse-height analyzer, which then displayed pulses from the central crystal of the spectrometer. The spectra thus measured at two angles of observation, 0 and 90 deg, are shown in Fig. 7. The peaks are labeled by the energies of the initial and final states to which they correspond. All the transitions, save the 2.00 → 0 transition in C^{11}, are assigned to N^{14}. The solid lines give the results of a computer fit discussed in the next section. In conclusion, it is estimated that the net error introduced into the measurement by experimental uncertainties is less than 2%.

C. Results

For each of the 5 angles of observation the data were analyzed, using the computer program described in Sec. IIIA, to determine the areas under the peaks corresponding to the various transitions. The computer fit to the data for two angles is shown by the solid lines of Figs. 7(a) and 7(b). The angular variations of intensities thus determined were fitted to an expansion in even-order Legendre polynominals of the form $W(\theta) = \Sigma_\nu A_\nu P_\nu(\cos\theta)$. The results are summarized in Table III. Columns 1 and 2 list, respectively, for each transition, the energies of the initial and final states in N^{14} and the gamma-ray energies (nominal). Relative intensities are listed in column 3. Solutions for the A_ν coefficients

TABLE III. Summary of gamma-ray angular distribution measurements for $C^{12}(He^3,p)N^{14}$ as obtained for a He^3 bombarding energy of 2.75 MeV. The transitions are labeled by the gamma-ray energies (nominal) and by the energies of the initial and final states in N^{14}. The relative intensities are given in arbitrary units. Solutions for the A_ν coefficients for a Legendre-Polynominal fit of the data are indicated by the ratios A_2/A_0 and A_4/A_0 for values $\nu_{max} \leq 4$.

Transition	$E\gamma$ (MeV)	Relative intensity	ν_{max}	A_2/A_0	A_4/A_0
6.21 → 0	6.21	4.1 ±0.6	2	−0.009 ±0.045	
5.69 → 0	5.69	17 ±1.5	2	0.139 ±0.023	
5.10 → 0	5.10	34 ±2.5	2	−0.110 ±0.023	
			(4)	−0.109 ±0.023	−0.007 ±0.026
4.91 → 0	4.91	9.5 ±1	2	−0.028 ±0.071	
6.21 → 2.31	3.90	10.5 ±1	2	0.031 ±0.048	
5.69 → 2.31	3.38	18.3 ±1.7	2	−0.325 ±0.031	
5.10 → 2.31	2.79	9.1 ±1	2	0.368 ±0.085	
			(4)	0.362 ±0.093	0.015 ±0.098
2.31 → 0	2.31	170 ±8	2	−0.002 ±0.014	
3.95 → 2.31	1.63	67 ±9	2	0.160 ±0.070	

[13] See, for example, H. DeWaard, Nucleonics **13**, 36 (1955).

are indicated in columns 4 and 5, which list the ratios A_2/A_0 and A_4/A_0. All of the data were fit for values $\nu_{max} \lesssim 2$. However, for the transitions proceding from the 5.10-MeV ($J=2$) level, which may give rise to terms in $P_4(\cos\theta)$, the solutions obtained for $\nu_{max}=4$ are also listed. Relative intensities were calculated from the A_ν values obtained by the computer fit using the pair-detection efficiency curve determined previously for Sec. IIA. Because the geometries for these measurements were not precisely the same, however, an estimated uncertainty of 5% has been incorporated into the values given in Table III to allow for a possible variance in the energy dependence of the product $\sigma_p(\Sigma_G/\Sigma_T)$.

Since the 2.31-MeV transition proceeds from a state of total angular momentum $J=0$ its angular distribution must necessarily be isotropic. The results listed in Table III which indicate $A_2/A_0 \lesssim 0.02$, therefore provide a satisfactory internal check on the accuracy of the experimental measurements. Similarly, the 4.91-MeV angular distribution must also be isotropic if the 4.91-MeV level is $J^\pi=0^-$ as assumed. It is noted in Figs. 7(a) and 7(b) however, that the 4.91- and 5.10-MeV lines were not experimentally resolved; further, the 4.91-MeV line experiences an appreciable Doppler shift, to the extent that it appears to be partially merged with the (unshifted)[10] 5.10-MeV line at the forward angle of 0 deg. This particular doublet, therefore, provides a useful test of the ability of the analysis to separate the unresolved peak into two components. The results given in Table III, which do indeed indicate isotropy for the 4.91-MeV transition, therefore, provide a satisfactory check on this phase of the analysis.

Following the outline presented in Sec. IVA the values determined for A_ν/A_0 were used to calculate the mixing parameters for those levels which decay to both the ground state ($J=1$) and to the 2.31-MeV state ($J=0$). Obviously, the approach will not work for the

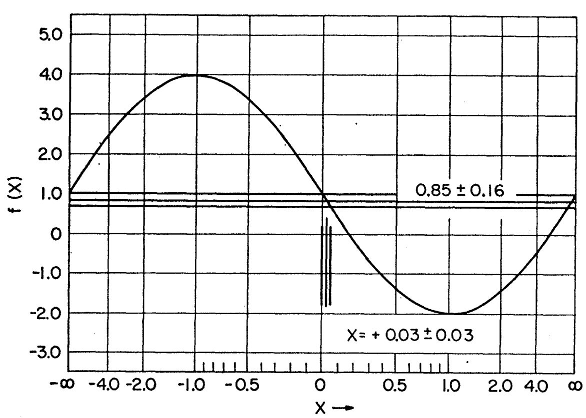

FIG. 8. The mixing parameter x for a transition between initial and final states with $J_i=J_f=1$ versus the function $f(x) = (1-6x+x^2)/(1+x^2)$. The experimentally determined value of $f(x)$ for the decay of the N^{14} 5.69-MeV level is 0.85 ± 0.16 and is indicated in the figure. This value of $f(x)$ is found to correspond to $x=+0.03\pm0.03$.

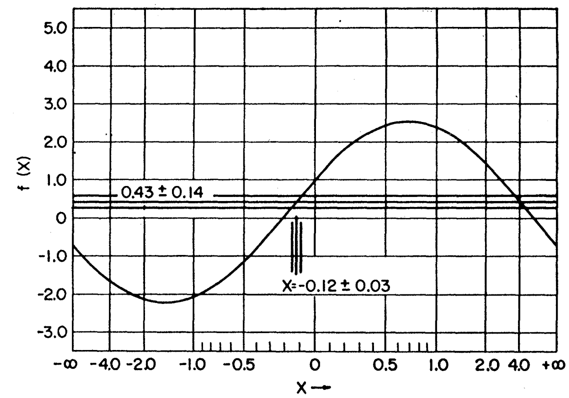

FIG. 9. The mixing parameter x for a transition between initial and final states with $J_i=2$, $J_f=1$ versus the function $f(x) = (1+4.472x-0.714x^2)/(1+x^2)$. The experimentally determined value of $f(x)$ for the decay of the N^{14} 5.10-MeV level is 0.43 ± 0.14 and is indicated in the figure. This value of $f(x)$ is found to correspond to $x=-0.12\pm0.03$.

6.21-MeV level, since both radiations are isotropic within the accuracy of the experimental measurement. However, for the 5.69- and 5.10-MeV levels, significant anisotropies were measured; the results of graphical solutions for the quadrupole to dipole mixing parameters x are presented in Figs. 8 and 9.

For the decay of the 5.69-MeV level $J_i=J_f=1$ and Eq. (5) applies. The solid curve of Fig. 8 shows a plot of the function $f(x)=(1-6x+x^2)/(1+x^2)$ defined by Eq. (5). The experimentally determined value for $f(x) = -2A_2(1,1)/A_2(1,0)=(0.85\pm0.16)$ is indicated. The solution for the quadrupole to dipole mixing parameter for the $5.69\rightarrow0$ ground-state transition is $x=(+0.03 \pm0.03)$.[14] An upper limit of 3.6×10^{-3} can, therefore, be set on the intensity of $M2$ radiation relative to the favored $E1$ radiation.

For the decay of the 5.10-MeV level, $J_i=2$, $J_f=1$. The solid curve of Fig. 9 shows a plot of the function $f(x)=(1+0.472x-0.714x^2)/(1+x^2)$ defined by Eq. (6). The experimentally determined value $f(x)=-(10/7) A_2(2,1)/A_2(2,0)=(0.43\pm0.14)$ is indicated as is the solution $x=(-0.12\pm0.03)$.

V. CONCLUSIONS

The $J^\pi=3^+$ 6.44-MeV state of N^{14} is found to decay by $E2$ radiation to the N^{14} ground state and 3.95-MeV level with branches of $(65\pm3)\%$ and $(21\pm2)\%$, respectively. There is also a $(14\pm3)\%$ branch to the $J^\pi=2^-$ 5.10-MeV level which is presumably $E1$. The positive identification of the $6.44\rightarrow3.95$ decay mode confirms earlier suspicions[6] that the 6.44-MeV level has a sizeable branch to the 3.95-MeV level. The lifetime of the N^{14} 6.44-MeV level has recently been measured by

[14] The results shown in Figs. 8 and 9 both allow two solutions for the mixing parameter x. However, in both cases the solution corresponding to the larger value of $|x|$ is ruled out by the fact that the $5.69\rightarrow0$ and $5.10\rightarrow0$ transitions are both predominantly $E1$ (see Ref. 2).

the Doppler shift attenuation method. The lifetimes of the three decay modes of the 6.44-MeV level are discussed in the report[9] of that measurement.

From a study of transition multipolarities the N^{14} 6.21-MeV level is shown to have $J^{\pi}=1^{+}$ and the even-parity assignment[3] for the 6.44-MeV level is confirmed. The spin-parity assignments for these two states are in agreement with shell-model calculations of True[15] who assigns these levels to the $s^4p^8(2s,1d)$ configuration; they are also in agreement with their other known properties.[16]

The method[10,11] of extracting information from studies of electromagnetic transitions emitted by a state J_i without recourse to knowledge of the mechanism of formations of the state J_i is applied to determining the amplitude ratio of quadrupole to dipole radiation for the N^{14} $5.69\rightarrow 0$ and $5.10\rightarrow 0$ transitions from gamma-ray angular distribution measurements alone. The results for the decay of the 1^- 5.69-MeV level and 2^- 5.10-MeV level to the 1^+ ground state are $x=+(0.03\pm0.03)$ and $x=-(0.12\pm0.03)$, respectively. The latter result is in fair agreement with an earlier determination[17] of $x=-(0.17\pm0.03)$ and we adopt $x=-(0.14\pm0.03)$ for the $5.10\rightarrow 0$ transition. We note that the analysis for the $5.10\rightarrow 0$ transition in both this work and the earlier work[17] was made assuming that the contribution of octupole radiation can be neglected. As discussed previously,[17] this assumption may not be valid in this case because of the inhibition of electric dipole and magnetic radiation for $\Delta T=0$ transitions in self-conjugate nuclei and the possible enhancement of electric octupole radiation.

The values of the mixing parameters obtained for the $5.10\rightarrow 0$ and $5.69\rightarrow 0$ transitions indicate that the contribution of $M2$ radiation to the $5.10\rightarrow 0$ transition is at least four times stronger than that for the $5.69\rightarrow 0$ transition. This is not surprising since the $E1$ $5.69\rightarrow 0$ transition, although forbidden by the isotopic-spin selection rule, must be quite strong in order to compete favorably with the allowed $5.69\rightarrow 2.31$ $E1$ transition, while on the other hand, the $E1$ $5.10\rightarrow 0$ transition is strongly inhibited as is shown by the fact that the lifetime of the 5.10-MeV state is greater than 3×10^{-13} sec.[17]

The branching ratios for transitions from the 5.10-, 5.69-, and 6.21-MeV levels of N^{14} to the ground state and 2.31-MeV level can be obtained from the relative intensities given in Tables I and III. The results obtained at the three bombarding energies used are in fair agreement. Averaging the three determinations for the branching ratios of these three levels we obtain branching ratios to the N^{14} ground state and 2.13-MeV level of $(75\pm3)\%$, $(25\pm3)\%$ for the 5.10-MeV level; $(40\pm3)\%$, $(60\pm3)\%$ for the 5.69-MeV level; and $(24\pm3)\%$, $(76\pm3)\%$ for the 6.21-MeV level. The results for the 5.69- and 6.21-MeV level are in good agreement with earlier measurements.[1,4] A previous determination for the N^{14} 5.10-MeV level decay was $(68\pm4)\%$ to the N^{14} ground state and $(32\pm4)\%$ to the N^{14} 2.31-MeV level,[17] in slight disagreement with the present values. Taking an average of the previous values with those of the present work gives $(72\pm3)\%$ and $(28\pm3)\%$ for the branches of the N^{14} 5.10-MeV level to the N^{14} ground state and 2.31-MeV level, respectively.

[15] W. W. True, Phys. Rev. **130**, 1530 (1963).

[16] E. K. Warburton and W. T. Pinkston, Phys. Rev. **118**, 733 (1960).

[17] E. K. Warburton, H. J. Rose, and E. N. Hatch, Phys. Rev. **114**, 214 (1959).